Bounds from multimessenger astronomy on the superheavy dark matter

M. Deliyergiyev,[1,*] A. Del Popolo,[2,3,†] and Morgan Le Delliou[4,5,6,‡]

[1]*Department of Nuclear and Particle Physics, University of Geneva, Geneva CH-1211, Switzerland*
[2]*Dipartimento di Fisica e Astronomia, University of Catania, Viale Andrea Doria 6, Catania I-95125, Italy*
[3]*Institute of Astronomy, Russian Academy of Sciences, 119017 Pyatnitskaya Street, 48, Moscow, Russia*
[4]*Institute of Theoretical Physics, School of Physical Science and Technology, Lanzhou University, No. 222, South Tianshui Road, Lanzhou, Gansu 730000, China*
[5]*Instituto de Astrofísica e Ciências do Espaço, Universidade de Lisboa, Faculdade de Ciências, Edificio C8, Campo Grande, 1769-016 Lisboa, Portugal*
[6]*Lanzhou Center for Theoretical Physics, Key Laboratory of Theoretical Physics of Gansu Province, Lanzhou University, Lanzhou, Gansu 730000, China*

(Received 18 March 2022; accepted 29 July 2022; published 6 September 2022)

The purely gravitational evidence supporting the need for dark matter (DM) particles is compelling and based on Galactic to cosmological scale observations. Thus far, the promising weakly interacting massive particles scenarios have eluded detection, motivating alternative models for DM. We consider the scenarios involving the superheavy dark matter (SHDM) that potentially can be emitted by primordial black holes (PBHs) and can decay or annihilate into ultrahigh-energy (UHE) neutrinos and photons. The observation of a population of photons with energies $E \geq 10^{11}$ GeV would imply the existence of completely new physical phenomena, or shed some light on DM models. Only the ultrahigh-energy cosmic-ray observatories have the capabilities to detect such UHE decay products via the measurements of UHE photon-induced extensive air showers. Using the upper bound on the flux of UHE cosmic rays beyond $10^{11.3}$ GeV implying $J(> 10^{11.3}\ \text{GeV}) < 3.6 \times 10^{-5}\ \text{km}^{-2}\ \text{sr}^{-1}\ \text{yr}^{-1}$, at the 90% C.L. reported by the Pierre Auger Observatory, we obtain global limits on the lifetime of the DM particles with masses $10^{15} \leq M_X \leq 10^{17}$ GeV. The constraints derived here are new and cover a region of the parameter space not yet explored. We compare our results with the projected constraints from future POEMMA and JEM-EUSO experiments, in order to quantify the improvement that will be obtained by these missions. Moreover, assuming that an epoch of early PBHs domination introduces a unique spectral break, f_*, in the gravitational wave spectrum, the frequency of which is related to the SHDM mass, we map potential probes and limits of the DM particles masses on the $f_* - M_X$ parameter space.

DOI: 10.1103/PhysRevD.106.063002

I. INTRODUCTION: SOURCES OF CONSTRAINTS ON *X* PARTICLES

The current cosmological understanding of structure formation, without taking the hazardous jump away from standard General Relativity gravity, implies postulating the existence of Dark Matter (DM). Such existence, which entails specific gravitational consequences on structures that have been well established [1,2], although cosmologically dominant, continues to fail to produce constituent particles events in direct detection attempts, whether through nuclear recoil tanks or in accelerators [3–13], or in indirect surveys seeking detection through annihilation events of weakly interacting massive particle (WIMP) [14].

So far, many fundamental characteristics of DM particles remain quite unconstrained, including their mass or their self-annihilation time. Solutions to problems of the particle physics Standard Model (SM) have given birth to a wealth of DM models. Although most of them keep DM in a separate noninteracting sector, none of the models have won over the favors of the field because of their compelling theoretical appeal.

For many decades, the favored models characterized DM as a relic density of WIMPs [15–18] (for a precise calculation of the WIMP relic abundance, see Refs. [19,20]; partial-wave unitarity dictates an upper bound on the WIMP mass ≤ 110 TeV). However, the extensive experimental program setup for WIMP detection in the direct and indirect detection experiments [21–33] as well as in the LHC has given negative or inconclusive results so far [34–36]. Despite these facts, a complete exploration of the WIMP

*maksym.deliyergiyev@unige.ch
†adelpopolo@oact.inaf.it
‡Morgan.LeDelliou.ift@gmail.com

parameter space remains the highest priority of the DM community, and WIMP discovery is still a viable option in next-generation experiments.

Because the assumption of relatively low-mass DM seems quite natural, it is rarely questioned. However, the null results from DM searches began closing the favored parameter space for the WIMP models and at the same time started to open a door to alternatives to the WIMP paradigm.

More recently, dark sector interactions have been given more serious consideration, the viability of which has been scrutinized in Comelli *et al.* [37]. Observational effects on galaxy clusters dynamics of such interactions have gathered credibility [38–46]. However, most of the current constraints tend to favor stable or long-lived, cold or warm, nonbaryonic DM [47]. They consequently prompted the exploration of improved interacting models that respect those constraints, opening fairly large mass and interaction strength ranges for acceptable DM candidates [48].

Alternative views on DM have emerged a while ago. The most radical of them suggests that DM interacts only gravitationally, explaining the negative experimental results. For example, cold DM could be a manifestation of the gravitational sector itself consisting of massive gravitons of bimetric gravity [49,50]—the only known self-consistent, ghost-free extension of General Relativity with massive spin-2 fields [51].

Among the well-motivated and less radical ideas for what DM could be, the WIMPzilla hypothesis postulates that DM is made of gravitationally produced (nonthermal relic) superweakly interacting supermassive so-called X particles—the superheavy Dark Matter (SHDM) [52–58]. The hypothesis of DM consisting of heavy long-lived particles has attracted significant attention in the context of inflationary cosmology [59–62]. There are several scenarios of effective DM particles production at various stages of early Universe evolution. SHDM can be created gravitationally at the end of inflation [52–54,61], during preheating [63,64] and reheating [59,65,66], and from the collisions of vacuum bubbles at phase transitions [55,64], or from emission [67] of the primordial black holes (PBHs) (see Ref. [57] for a review).

Of course, SHDM particles have been considered before to a certain extent. In particular, there is an extensive literature regarding observational constraints on unusually heavy DM candidates [for example, see Refs. [68–71], and references therein]. The earliest observational hint of SHDM existence was provided in the AGASA experiment by detection of superGZK cosmic rays [[72] with GZK standing for Greisen, Zatzepin, and Kuzmin]. This GZK cutoff was later supported in results from next-generation cosmic-ray experiments [73,74]. The IceCube PeV neutrinos detection [75,76] have led to various DM decay propositions of interpretations [77–82]. However, recent analyses of the respective γ-ray signal [83,84] have deprecated most of them, although the photon production suppression feature of a few of those DM models keep them conceivable [80,85,86]. The ultrahigh-energy cosmic rays (UHECRs) flux appears, from experimental data, to be dominated, above its "ankle," by an astrophysical, extragalactic component [87], most possibly sourced from starburst galaxies [88]. Supposing the systematic uncertainties of current high-energy hadronic interaction models remain sufficiently small, we can expect the acceleration of heavier nuclei, in addition to protons, as sources of this flux. Nevertheless, experimental data still allow for a minority component of different origin which, beyond the suppression, could still dominate the flux [71,89].

The possibility that the by-products of the decay of unstable SHDM particles can contribute to the UHECR flux has been studied extensively in the past [see for instance Refs. [90–95]]. In these models, DM is composed of supermassive particles produced gravitationally during inflation [52–54,57]. These particles would be clustered in the halo of the galaxies, such as ours.

The discovery of gravitational waves (GWs) by Laser Interferometer Gravitational Wave Observatory (LIGO) and Virgo Collaboration of black holes [96–100] and neutron stars [101,102] has opened up a new cosmic frontier for the SHDM search by examination of the stochastic GW background (SGWB) [103–106] in the multifrequency range [67].

Two main problems should be addressed in the discussion of SHDM models: how particles with very high mass ($M_X > 10^{13}$ GeV) can be quasistable, with a lifetime much longer than the age of the Universe t_0, and how their abundance can be dominant in the Universe today. The stability of SHDM can be achieved assuming the existence of a discrete gauge symmetry that protects the particle from decaying, in the same way as neutralino stability through R parity in supersymmetry. This discrete symmetry can be weakly broken, assuring a lifetime $\tau_X > t_0$, through wormhole [60] or instanton [59] effects. An example of a particle with a lifetime exceeding the age of the Universe can be found in [107]. Instanton decays induced by operators involving both the hidden sector and the SM sector may give rise to observable signals in the spectrum of UHECRs [59,60]. Another possible way to stabilize such particles may be a modification of the standard cosmological expansion law in such a way that the density of these heavy relics would be significantly reduced [108].

Therefore, technically the SHDM models have two main parameters: mass M_X and lifetime, τ_X, in which a minority component of the UHECRs originates from the decay of these unstable particles. Stable X particles are not so interesting from the experimental point of view since their annihilation cross section is bounded by unitarity: $\sigma_X^{\mathrm{ann}} \sim 1/M_X^2$, which makes its indirect detection impossible for today's experiments [109]. The spectrum from SHDM decay is expected to be dominated by gamma rays

[110–112] and neutrinos [77,113] because of more effective production of pions than nucleons in the QCD cascades. Since the photons would not be attenuated owing to their proximity, they become the prime signal because it is easier to detect photons than neutrinos. However, such γ-ray production can be substantially different for different decay channels [71].

While it is very challenging to probe such superheavy DM via the traditional direct, indirect, or collider experiments, this paper aims to show the current bounds on such X particles, with a mass larger than the weak scale by several (perhaps many) orders of magnitude, from the perspective of the recent cosmic-ray and GW observations. In this paper, we examine particles' mass range from 10^{15} to 10^{17} GeV together with the most recent UHECR and GW data to derive the strongest lower limit on the lifetime of decaying superheavy WIMPs (WIMPzillas) and their mass. In Sec. II we estimated the photon flux from SHDM decays. For this, we evaluated two separate contributions: the astrophysical factor and the particle physics factor. We used current high-energy γ-ray measurements [114] to examine bounds that one may put on the parameter space of decaying SHDM. In addition, from the relation of the GW spectrum break, f_*, with the SHDM mass, following Ref. [67], we mapped potential probes and limits of the SHDM particle masses on the $f_* - M_X$ parameter space in Sec. III. Result discussion is given in Sec. IV and we conclude in Sec. V.

II. BOUNDS ON SHDM FROM THE γ-RAY FLUX

Given the mass of the SHDM particles, the decay time corresponding to the scenario for the largest SHDM cosmic-ray flux, compatible with the upper limits to the photon fraction obtained by the Pierre Auger Observatory (PAO), can be estimated from the predicted integral γ-ray flux [110], which may be observed on Earth by an observatory with uniform exposure, as

$$J(E) = \frac{N(E > E_{\rm min})}{4\pi M_X \tau_X} \left\{ \frac{\int_V \frac{\rho_{\rm DM}(r)\omega(\delta, a_0, \theta_{\rm max})}{r^2} dV}{2\pi \int_{-\frac{\pi}{2}}^{\frac{\pi}{2}} \omega(\delta, a_0, \theta_{\rm max}) \cos(\delta) d\delta} \right\}. \tag{1}$$

This expression can be easily adopted in case we start to look at cosmic rays using the Moon's regolith [115]. Here $N(E > E_{\rm min})$ is an integral number of photons with energies higher than $E_{\rm min}$ produced in the decay of X particle; θ is the angle between the line of sight and the axis defined by Earth and the Galactic center [116]; τ_X is the SHDM lifetime, 10^{11}–10^{22} years; M_X is the SHDM particle mass, 10^{15}–10^{17} GeV; $\rho_{\rm DM}(r) \equiv \rho_X(r)$ is the density of DM in the Galaxy as function of distance, r, from the Galactic Center, in $\frac{\rm GeV}{\rm cm^3}$. Integration in the numerator ranges over all the volume of the halo ($R_H = 260$ kpc) and in the denominator over all the sky [the averaging over right ascension is included in the definition of the directional exposure, $\omega(\hat{\mathbf{n}})$].

The directional exposure, $\omega(\hat{\mathbf{n}})$, provides the effective time-integrated collecting area for a flux from each direction of the sky $\hat{\mathbf{n}}(\alpha, \delta)$, characterized by the right ascension α and the declination δ. For an experiment at latitude λ, which is fully efficient for particles arriving with zenith angle $< \theta_{\rm max}$ and that experiences stable operation, $\omega(\hat{\mathbf{n}})$ actually becomes independent of α when integrating the local-angle detection efficiency over full periods of sidereal revolution of the Earth. Full efficiency means that the acceptance depends on θ only through the reduction in the perpendicular area given by $\cos(\theta)$. The ω dependence on declination, δ, geographical latitude of the given experiment λ, and the maximal zenith angle $\theta_{\rm max}$ accessible for fully efficient observation in the experiment, rely on geometrical acceptance terms and is given by [117,118]

$$\omega(S, \Delta t, \delta, \lambda, \theta) = \frac{S\Delta t}{2\pi} \cos(\lambda) \cos(\delta) \sin(a_m(\theta, \delta, \lambda)) + \frac{S\Delta t}{2\pi} a_m(\theta, \delta, \lambda) \sin(\lambda) \sin(\delta), \tag{2}$$

where S is the effective surface of the given experiment (detector array); Δt is the total exposure time of the given experiment (or time of data collection). The location of the Pierre Auger Observatory, $35.1° - 35.5°$S, $69.6°$W at 875 g/cm^2 atmospheric depth [119], corresponds to the Pampa Amarilla plain, in the Mendoza Province of Argentina, close to the Malargüe town. Initiating data collection in January 2004 and completing its baseline design construction by 2008, by 2021 the PAO collected exposure had exceeded 7.68×10^4 km^2 sr yr, exceeding the sum over all of the other cosmic-ray experiments available [120]. Therefore, for the PAO with $S = 1.037 \times 10^4$ km^2, $\Delta t = 7.41$ yr from Ref. [120], $\lambda = -35.2°$ and $-15° \leq \delta \leq 25°$.

The parameter a_m of the observatory is given by

$$a_m(\theta, \delta, \lambda) = \begin{cases} 0 & \text{for } \xi > 1 \\ \pi & \text{for } \xi > -1 \\ \arccos(\xi) & \text{otherwise,} \end{cases}$$

with

$$\xi(\theta, \delta, \lambda) = \frac{\cos(\theta_{\rm max}) - \sin(\lambda)\sin(\delta)}{\cos(\lambda)\cos(\delta)}. \tag{3}$$

The DM galactic distribution, or DM density profile $\rho_{\rm DM}$, is a function of the Galactic longitude, l, and latitude b, which in turn is related to the line-of-sight, s, coordinate:

$$r(s, b, l) = \sqrt{s^2 + r_\odot^2 - 2 s r_\odot \cos(b)\cos(l)}, \tag{4}$$

where $r_\odot = 8.5$ kpc denotes the distance between the Earth and the Galactic Center. The local DM density is an important ancillary parameter when constraining DM signatures. However, due to the lack of a robust estimate of ρ_X, the distribution of DM is assumed to follow a density profile inspired by numerical simulations, typically an analytic fit such as the well-known Navarro-Frenk-White (NFW) [121] or Einasto [122,123] profiles, with two or more free parameters whose best-fit values are then determined from dynamical constraints. In this work we adopt both reference profiles: the NFW profile

$$\rho_X^{\mathrm{NFW}}(r) = \rho_s \left[\frac{r}{r_s}\left(1+\frac{r}{r_s}\right)^2\right]^{-1} \tag{5}$$

with $r_s = 28.44$ kpc [121], and the Einasto profile

$$\rho_X^{\mathrm{Einasto}}(r) = \rho_s e^{-\frac{2}{\alpha}[(\frac{r}{r_s})^\alpha - 1]}, \tag{6}$$

in contrast with the somewhat steeper NFW profile, with $r_s = 30.28$ kpc, $\alpha = 0.17$ [122,124], and $\rho_s = 0.105$ GeV cm^{-3} [89]. Most recent systematic efforts to estimate a proper DM profile were summarized in Ref. [125].

With all this in hand, and defining the element of Galaxy volume in Eq. (1) as

$$dV = r^2 \sin(\varphi) dr d\varphi d\theta = r^2 \sin\left(\frac{\pi}{2} - \delta\right) dr d\delta d\theta, \tag{7}$$

one can rewrite the flux expression (1) as follows:

$$J(E) = \frac{1}{4\pi}\frac{1}{M_X \tau_X}\frac{dN}{dE}\left\{\frac{\int_0^{50\mathrm{kpc}} \frac{\rho_X(r)}{r^2} r^2 dr \int_{-\frac{\pi}{2}}^{\frac{\pi}{2}} \sin(\frac{\pi}{2}-\delta) d\delta \int_0^{2\pi} \frac{\omega(\delta, a_0, \theta_{\max})}{1} d\theta}{2\pi \int_{-\frac{\pi}{2}}^{\frac{\pi}{2}} \omega(\delta, a_0, \theta_{\max}) \cos(\delta) d\delta}\right\}. \tag{8}$$

Using the radius of the Galactic halo $R_H = 260$ kpc, the integral in Eq. (8) can be split into two integrals as was shown in Refs. [89,126]:

$$J(E,\theta) = \frac{1}{4\pi}\frac{1}{M_X \tau_X}\frac{dN}{dE}\left\{2\int_{r_\odot \sin\theta}^{r_\odot} r \frac{\rho_X(r)}{\sqrt{r^2 - r_\odot^2 \sin^2\theta}} dr + \int_{r_\odot}^{R_H} r \frac{\rho_X(r)}{\sqrt{r^2 - r_\odot^2 \sin^2\theta}} dr\right\}. \tag{9}$$

Therefore, the expected energy distribution on Earth follows the initial decay spectrum, whereas the angular distribution incorporates the (uncertain) distribution of DM in the Galactic halo via the line-of-sight integral [91,94,127,128].

The energy spectrum, dN/dE, of the expected gamma rays depends on the exact SHDM decay mechanism and is model dependent. In our computation we used the following flat spectrum similar to [89]:

$$\frac{dN(E)}{dE} \sim \cos(\delta)\omega(S, \Delta t, \delta, \lambda, \theta)\left[M_X^{0.9} \log\left(\frac{2E}{M_X}\right)^{-1.9}\right], \tag{10}$$

validated for $X \to q\bar{q}$ decay, it is independent of the particle type, assuming the photon/nucleon ratio is $2 \lesssim \gamma/N \lesssim 3$ and the neutrino/nucleon ratio is $3 \lesssim \nu/N \lesssim 4$. In comparison with the other spectra available in the literature [129–132], the spectrum from [89] is much flatter. This allows one to have fixed photon/nucleon and neutrino/nucleon ratios along the whole energy range. The consideration of the bosonic decay channels such as WW/ZZ/hh, or leptonic $ee/\mu\mu/\tau\tau$ would require a different stable particle spectra in Eq. (9).

The PAO is composed of two types of instruments: (a) fluorescence telescopes, that measure light from atmospheric nitrogen excitation by air shower particles, and (b) ground particle detectors, that sample air shower fronts arriving at the Earth's surface. Its maximum zenith angle falls at $\theta_{\max} = 90°$, with the downward-going (DG) channel constrained to $60° \leq \theta \leq 90°$ while the Earth-skimming (ES) channel extends to $60° \leq \theta \leq 95°$ [see Ref. [133]]. Therefore, in order to make a direct comparison with current limits on the diffuse UHE γ-ray flux, from Eq. (9), following [110], we compute the angle-averaged integral γ flux over the whole sky $(0 < \theta < \pi)$, averaging over the directional exposure at the declination of the Auger Observatory, where the declination limits are $-15° \leq \delta \leq 25°$ [118].

The SHDM flux contributions from the extragalactic and galactic halos need to be resolved as they can be important due to the fact that the gamma rays and protons originating in that extragalactic halo come from a narrow region of the sky. Therefore, in that region the contribution of the extragalactic halo can be more important than the one corresponding to our galaxy, especially in regions far from the galactic center where the galactic contribution decreases considerably [126].

TABLE I. Integral fluxes for the DM particle candidates with mass, M_X. DM fluxes computed with the help of Eq. (9) assuming the Einasto and NFW DM density profiles. In addition, we show results obtained with the energy spectra from [129,130].

M_X, (GeV)	τ_X, (years)	$J(>E_0)$	τ_X, (years)	$J(>E_0)$
	Einasto, $r_s = 30.28$ kpc			
10^{15}	10^{21}	6.803×10^{-5}	10^{22}	6.803×10^{-6}
10^{16}	10^{21}	7.406×10^{-5}	10^{22}	7.406×10^{-6}
10^{17}	10^{21}	8.571×10^{-5}	10^{22}	8.571×10^{-6}
10^{15} [129]	10^{21}	1.028×10^{-3}	10^{22}	1.028×10^{-4}
10^{16} [129]	10^{21}	3.250×10^{-3}	10^{22}	3.250×10^{-4}
10^{17} [129]	10^{21}	1.028×10^{-2}	10^{22}	1.028×10^{-3}
10^{15} [130]	10^{21}	5.867×10^{-4}	10^{22}	5.867×10^{-5}
10^{16} [130]	10^{21}	1.855×10^{-3}	10^{22}	1.855×10^{-4}
10^{17} [130]	10^{21}	5.867×10^{-3}	10^{22}	5.867×10^{-4}
	NFW, $r_s = 28.44$ kpc			
10^{15}	10^{21}	7.736×10^{-5}	10^{22}	7.736×10^{-6}
10^{16}	10^{21}	8.112×10^{-5}	10^{22}	8.112×10^{-5}
10^{17}	10^{21}	8.186×10^{-5}	10^{22}	8.186×10^{-5}
10^{15} [129]	10^{21}	2.047×10^{-4}	10^{22}	2.047×10^{-5}
10^{16} [129]	10^{21}	6.473×10^{-4}	10^{22}	6.473×10^{-5}
10^{17} [129]	10^{21}	2.047×10^{-3}	10^{22}	2.047×10^{-4}
10^{15} [130]	10^{21}	1.168×10^{-4}	10^{22}	1.168×10^{-5}
10^{16} [130]	10^{21}	3.694×10^{-4}	10^{22}	3.694×10^{-5}
10^{17} [130]	10^{21}	1.168×10^{-3}	10^{22}	1.168×10^{-4}
	NFW, $r_s = 30.28$ kpc			
10^{15}	10^{21}	5.451×10^{-5}	10^{22}	5.451×10^{-6}
10^{16}	10^{21}	5.675×10^{-5}	10^{22}	5.675×10^{-6}
10^{17}	10^{21}	5.988×10^{-5}	10^{22}	5.988×10^{-6}

The fluxes obtained for the various DM masses and DM density profiles are listed in Table I.

III. BOUNDS ON SHDM FROM THE GRAVITATIONAL WAVES OBSERVATIONS

Today, the scientific community has started to synthesize the various astronomical messengers, namely photons, neutrinos, cosmic rays, and gravitational waves. While photons, neutrinos, and cosmic rays still have a vital role to play in multimessenger astronomy, GW observation with pan-spectral electromagnetic radiation has enriched our understanding of violent astronomical events [101].

The details of the SHDM production mechanism can leave their footprint on the primordial GW amplitude as well as the spectral features. However, such a scenario is only present if DM mass would be generated by spontaneous symmetry breaking of an Abelian symmetry, which is not the general case.

An early Universe cosmological phase transition induced by this spontaneous symmetry breaking [134] may result in emergence of a cosmic-string network [135,136]—linelike topological defects. Cosmic strings restore that broken Abelian symmetry at the core of these topological defects with vortex types of behavior [137]. Their network loses energy through the shrinking of its closed loops following their emission of GWs [138,139]. The resulting primordial GW signal contains key signatures of ultraviolet physics that would otherwise remain far beyond the reach of regular ground detection. This is why such signal is a main focus of current and future investigations of the SGWB [103–106]. In addition, observation of such a signal [140–142] can be a complementary probe to the range of SHDM mass if one assumes that such DM particles are produced by emission of the PBHs.

The shape of the GW spectrum from a cosmic-string network is expected to follow a convex cored power law, the slope of which varies with amplitude and frequency, as well as is parametrized by the product $G\mu$ between the string tension μ and Newton's gravitation constant G.

The standard form of the spectral GW energy density can be expressed today as the power law:

$$\Omega_{\rm GW}(f) = \frac{2\pi^2}{3H_0^2} A^2 f_{\rm yr}^2 \left(\frac{f}{f_{\rm yr}}\right)^{5-\gamma_N}, \tag{11}$$

where f is the oscillation frequency of the emitted GWs, $f_{\rm yr} = 1\ {\rm yr}^{-1}$, A is the characteristic GW strain amplitude, γ_N is the spectral index of the pulsar timing–residual cross-power spectrum, and $H_0 = 67.7$ km/(Mpcs) is the present Hubble constant.

Following the recipe defined in [67] one can approximately determine the frequency at which the GW spectrum, $\Omega_{\rm GW}(f)h^2$, changes slope from a plateau described by f^0 to $f^{-1/3}$ with the help of the following expression:

$$f_* \simeq 2.1 \times 10^{-8} \sqrt{\frac{50}{z_{eq}\alpha\Gamma G\mu}} \left(\frac{M_X}{T_0}\right)^{\frac{3}{5}} T_0^{-\frac{2}{5}} t_0^{-1}, \tag{12}$$

where $\Gamma \simeq 50$ is the constant rate of GW radiation, $\alpha = 0.1$ characterizes the cosmic-string loop size at the time of formation, $z_{eq} = 3387$ is the redshift at the usual matter-radiation equality, occurring at the time t_{eq}, $T_0 = 2.725$ K is the photon temperature today, and $t_0 = 13.81$ Gyr is the age of the Universe.

With Eq. (12) we computed the turning-point frequencies, f_*, for the range of masses $M_X = 10^{12}$–10^{17} GeV assuming the dimensionless combination [67,143] between the corresponding cosmic-string tension and SHDM particle mass,

$$G\mu \sim GM_X^2. \tag{13}$$

The obtained frequencies lie within the range from 2.16 to 0.021 Hz, for masses ranging from 10^{12} to 10^{17} GeV, respectively. With such an assumption, furthermore admitting that the $G\mu$ value for $M_X = 10^{16}$ GeV is below the Cosmic Microwave Background (CMB) limit on $G\mu$ [144]

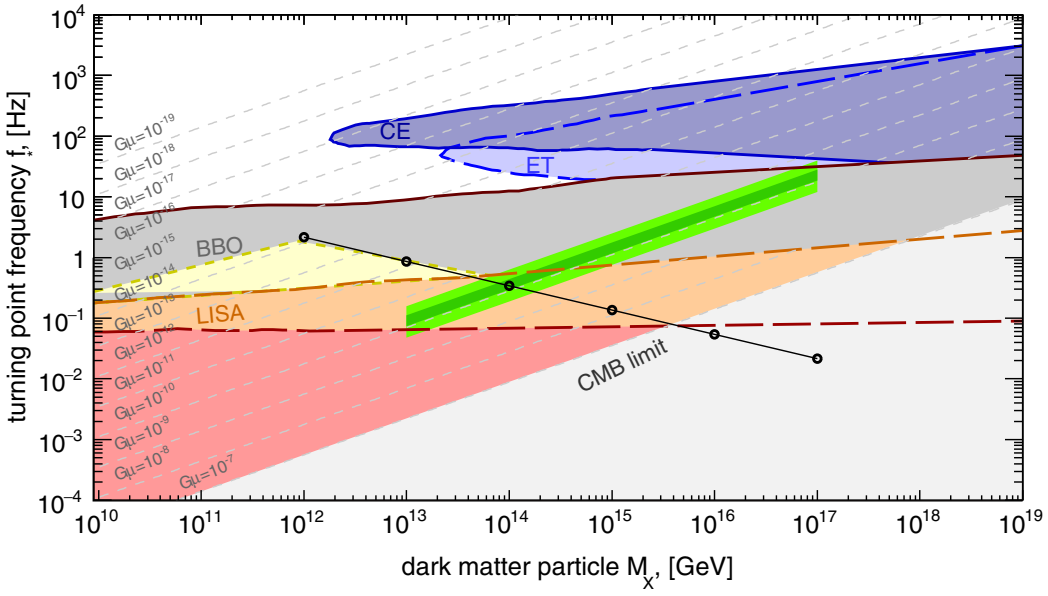

FIG. 1. Map of the possible probes of M_X and hence of the PBH evaporation temperature projecting the turning-point frequencies f_*, Eq. (12), for the various SHDM particle masses. Here, each diagonal line corresponds to the $G\mu$ value in the range 10^{-19} to 10^{-7} running from top to bottom. Below $G\mu = 10^{-7}$ lies the CMB limit for the cosmic string tension [145]. The relevant sensitivity curves of current or future GW detectors, such as the Einstein Telescope (ET), Cosmic Explorer (CE), LISA [146], and BBO [147], are reproduced from [67] using Eq. (12). The light-yellow region is the allowed parameter space assuming the PHB emission to SHDM scenario from [67]. The dark- and light-green bands denote the predicted turning-point frequencies computed assuming the 1σ and 2σ prediction on $G\mu$ parameter taken from [144] obtained from the fits to the NANOGrav data [140] for the examined SHDM particle masses.

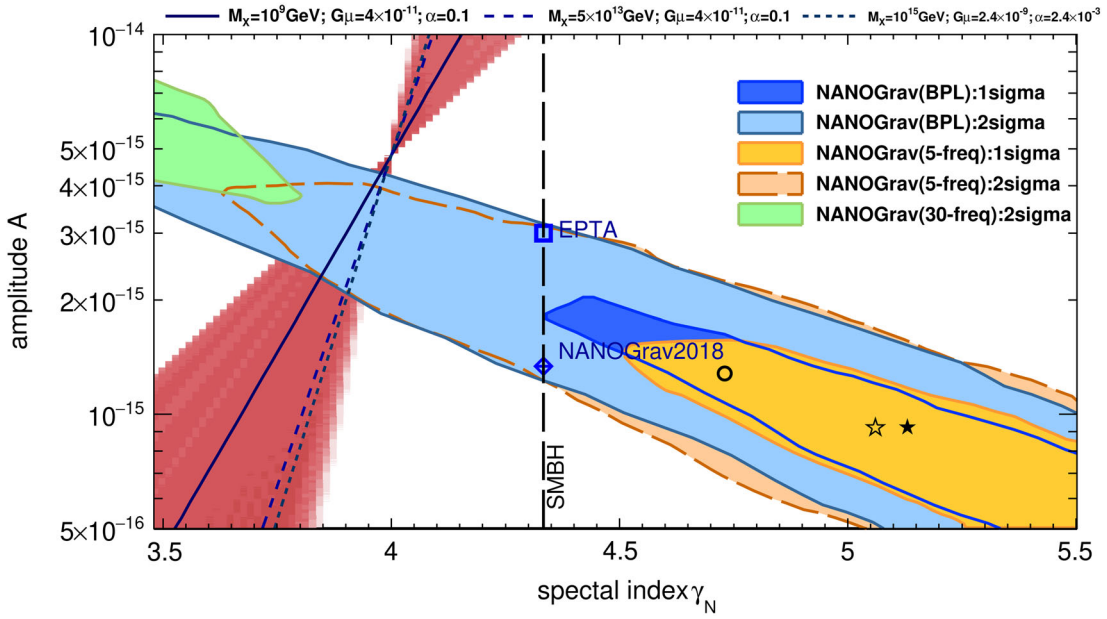

FIG. 2. The red graded area represents solutions of Eq. (14) with respect to the characteristic GW strain amplitude, A, at $f = f_*(M_X)$, projected onto the γ_N-A plane. Three benchmark points for A and γ_N parameters, which were listed in Ref. [144], are shown as markers (circle, shaded star, star). The dark and light contours denote the 1σ and 2σ posteriors in the NANOGrav analysis that allow to describe the observed stochastic process. Here, we use the contours taken from Ref. [140]. The black dashed vertical line indicates the theoretical prediction for a population of supermassive black hole binaries, $\gamma_N = 13/3$. Points on the vertical line denote a 95% upper limit on the dimensionless strain amplitude $A = 3 \times 10^{-15}$ and $A = 1.34 \times 10^{-15}$ at a reference frequency of 1 yr^{-1} and a spectral index of $13/3$ obtained from the European Pulsar Timing Array data and from the NANOGrav report, respectively [141,142].

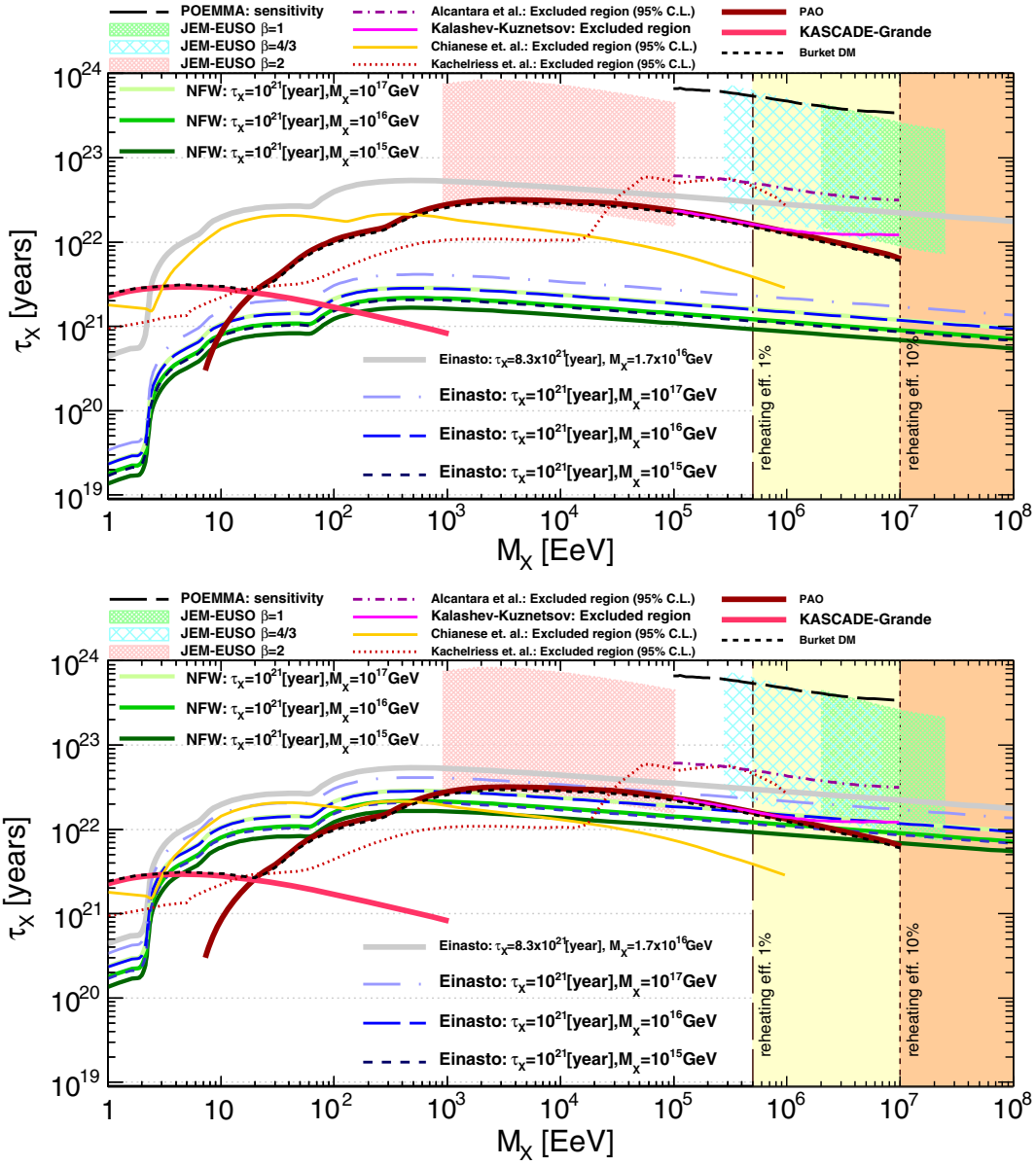

FIG. 3. Comparison of the upper constraints obtained in the literature with the 95% C.L. exclusion plot for mass M_X and lifetime τ_X of DM particles. The constraints that were obtained with the data of Pierre Auger full-sky analysis [148] assuming NFW DM profile (solid green lines), or with assumption that the DM profile is given by the Einasto model (dashed blue lines), constraints obtained using the DM flux estimation from Mikhail Kuznetsov given in the Ref. [89], are shown with the gray bold solid line. The lower limit on the lifetime of SHDM particles together with the stereoscopic τ_x sensitivity (defined by the observation of one photon event above $10^{11.3}$ GeV in 5 yr of data collection) of POEMMA (dashed dark gray line) was taken from [89]. The Alcantara 95% C.L. excluded region (dashed-dotted dark magenta line) and the Kalashed-Kuznetsov excluded region (solid magenta line), curves are all taken from [89]. The regions accessible to the JEM-EUSO experiment, each region corresponding to a different choice of the power-law index in the inflation potential, $\beta = 2; 4/3; 1$, are plotted from left to right [93]. The γ-ray limits placed by Chianese *et al.* [71] (orange solid line) and the limits placed by Kachelriess *et al.* [113] (red dotted line) are also shown. For illustration purposes, the 95% C.L. upper limit on mass obtained from the possible value of the Hubble rate at the end of inflation for a reheating efficiency of 1% (10%) is shown as the vertical dashed (dotted) line [149]. The constraints derived from diffuse γ-ray and neutrino limits from the PAO (solid bold dark red line) and from the KASKADE-Grande (solid bold red line) are shown. We also show for comparison the constraints obtained assuming Burkert DM profile (black short dashed line) using the data of Pierre Auger partial-sky analysis [148].

(see black data points in Fig. 1) while taking the resulting 1σ value of $G\mu$ [144] from the fits to the NANOGrav signal [140], which is $[4, 9] \times 10^{-11}$, we determined f_* in the range of 1.76(1.17) to 27.94(18.63) Hz. This result is shown with the green band in Fig. 1 with the different probes of the M_X and hence the PBH evaporation temperature. Assuming that PBHs evaporation causes a break in the GW spectrum at the turning-point frequency [67],

$f_*(M_X)$, from Eqs. (11) and (12) one may solve the following equality:

$$2.1\times10^{-8}\sqrt{\frac{50}{z_{eq}\alpha\Gamma G\mu}}\left(\frac{M_X}{T_0}\right)^{\frac{3}{5}}T_0^{-\frac{2}{5}}t_0^{-1} = \frac{2\pi^2}{3H_0^2}A^2f_{\rm yr}^2\left(\frac{f_*(M_X)}{f_{\rm yr}}\right)^{5-\gamma_N}, \quad (14)$$

with respect to the characteristic GW strain amplitude, A, by scanning over γ_N in the range of 3.5 to 5.5 with the step size of 0.005, $G\mu$ in the range of 10^{-12} to 10^{-7} with the step size of 10^{-13}, and α in the range of 10^{-6} to 0.2 with the step size of 0.025. The obtained solutions are compared with the NANOGrav observation in Fig. 2, where the red cone represents the domain of solutions for the mass range of $M_X = 10^9$–10^{19} GeV. The results for the benchmark values of $G\mu$ and α parameters, which are listed in [144], are shown with the solid and dashed blue lines to guide the eye.

IV. RESULTS AND DISCUSSION

The integral fluxes of photons at the location of the Auger Observatory for the different masses of the DM particle candidates are shown in Table I.

In Fig. 3 we compare the result of this work with the current lifetime limits placed by PAO, the KASCADE-Grande observations [89]. We add the existing γ-ray limits placed by Chianese *et al.* [71] (orange solid line) and Kachelriess *et al.* [113] (red dotted line). We also project the sensitivity regions for the future POEMMA, JEM-EUSO space missions. The regions accessible by the POEMMA experiment are shown with the dashed black line [89]. The regions accessible to the JEM-EUSO experiment, each region corresponding to a different choice of the power-law index in the inflation potential, $\beta = 2; 4/3; 1$, are plotted from left to right [93].

We see that the integral DM flux for the examined range of the DM particle candidate masses is of order 10^{-5}; see Table I. With such a DM flux, the examined SHDM particle candidates with masses of 10^{15}–10^{17} GeV and lifetime of 10^{21} yr may be already excluded by the current γ-ray observations; see Fig. 3 (top). In the case that some mechanisms could increase the DM flux by an order of magnitude with the same lifetime, small regions on the $\tau_X - M_X$ parameter space could then be constrained, but only by future detectors, such as JEM-EUSO, POEMMA; see Fig. 3 (bottom). The constraints obtained using the DM flux estimation from Kuznetsov given in Ref. [89] are shown with the gray solid line.

We estimate that the value of the GW spectral break, which can be computed from the SHDM particle mass, could represent the smoking gun in the indirect searches for the SHDM with a certain mass. It is exciting that the GW spectral break, f_*, for the range of the examined SHDM masses would be precisely within the sensitivity ranges of midband detectors such as BBO and LISA; see Fig. 1.

In Fig. 2 we map the extracted characteristic GW strain amplitude, A, by scanning the spectral index of the pulsar timing–residual cross-power spectrum, γ_N, using Eq. (14) on the recent finding of a stochastic common-spectrum process by NANOGrav. No matter what prior assumption we made on the initial values of SHDM mass, $G\mu$, α all obtained solutions intersect at the same value of the spectral index, $\gamma_N \simeq 4$. The slope of the lines in Fig. 2 is driven by the choice of M_X and $G\mu$. For $G\mu$ we took the obtained 1σ and 2σ $G\mu$ from the fits to NANOGrav data [144].

V. SUMMARY AND CONCLUSION

The abundance of SHDM can easily be dominant in the Universe today, with an SHDM density $\Omega_{\rm SHDM} \sim \Omega_{\rm DM}$. This effect can be obtained by gravitational production that resembles the production of density fluctuations during inflation. The gravitational production of particles during inflation [58,62] is the only experimentally verified DM production mechanism as the observed CMB fluctuations have exactly the same origin. This is because the production of SHDM during inflation gives rise to isocurvature perturbations that become sources of gravitational potential energy contributing to the tensor power spectrum of the CMB [150]. This implies a detectable primordial tensor-to-scalar ratio r in the CMB power spectrum. At the end of inflation, a fraction of fluctuations are not stretched beyond the horizon but remain as particles because the inflation slows down. The weakness of gravitational interaction naturally explains the tiny initial abundance of WIMPzillas [55]. Indeed, for such an abundance to be cosmologically relevant today, the X particles must be supermassive. The combined [Ade *et al.* [151], Planck satellite, together with Ade *et al.* [152], BICEP2 and the Keck array] 95% C.L. upper bound, $r < 0.07$, already constrains the X-particle mass to be $M_X \lesssim 10^{17}$ GeV in the limit of instantaneous reheating [149]. For slightly less efficient reheating, this upper limit strengthens to $M_X \lesssim 10^{16}$ GeV.

There are several sources of constraints for the SHDM parameters. In the energy range of interest the mass, M_X, and lifetime, τ_X, are constrained by cosmic-ray observations. The mass is subjected to cosmological constraints [52,54,55,57,150,153] and GW observations [67]. The lifetime of the DM particles can be effectively constrained with the observed fluxes of various high-energy particles or with the upper limit on these fluxes. The upper limits to the γ-ray flux obtained by Auger [110] and the non-detection of events above $10^{11.3}$ GeV by Auger impose tight constraints [89] to the flux corresponding to this hypothetical SHDM component; see dark red bold line in Fig. 3. The strongest limits for DM masses smaller

than $\sim 10^9$ GeV are obtained from KASCADE-Grande [71]; see red bold line in Fig. 3. In [154] the constraints (see thin magenta solid line in Fig. 3) have been placed using the shape of charged cosmic-ray spectra. However, with the modern cosmic-ray data this method is not as effective in constraining τ_X as neutrino [83,84] and γ-ray [84,93,110–112] data. Some fingerprints of the SHDM on GW signal were discussed in [67,143].

In the present paper, we have investigated the hypothesis of SHDM as a source of a subdominant component in the observed UHECR flux. The SHDM hypothesis is a viable candidate for DM in the Universe. Due to the expected small flux from the decay of SHDM particles, the studies in this paper have been done in the context of the next generation of UHECR observatories, POEMMA, JEM-EUSO, and ZAP [115], which are planned to have larger exposures compared with current ones. The limits obtained assuming the NFW DM profiles are weaker than those assuming the Einasto profiles. Given reports made in [71], this makes NFW limits the loosest among commonly used DM distributions.

Taking into account all currently available constraints in the literature on the SHDM, one may conclude that if the DM flux is around 10^{-5} km^{-2} sr^{-1} yr^{-1} for masses in the range 10^{15}–10^{17} GeV independently on the decay channel such SHDM hypothesis can be excluded. However, if there is some mechanism that may increase that flux by at least one order of magnitude, then there remains a window of opportunities to find these particles on the future POEMMA, JEM-EUSO, and ZAP experiments.

Since the examined DM mass range significantly exceeds the sensitivity regions of the traditional DM detection experiment, in view of the recent proposals [67,143] to search for the SHDM via GW astronomy we put bounds on the possible DM signal probes with such detection technique.

ACKNOWLEDGMENTS

We thank Luis Anchordoqui and Olivier Deligny for useful comments regarding the SHDM flux and constraints estimation. M. Le. D. acknowledges the financial support by the Lanzhou University starting fund, the Fundamental Research Funds for the Central Universities (Grant No. lzujbky-2019-25), the National Science Foundation of China (Grant No. 12047501), and the 111 Project under Grant No. B20063.

[1] M. Betoule *et al.* (SDSS Collaboration), Improved cosmological constraints from a joint analysis of the SDSS-II and SNLS supernova samples, Astron. Astrophys. **568**, A22 (2014).
[2] P. A. R. Ade *et al.* (Planck Collaboration), Planck 2013 results. XVI. Cosmological parameters, Astron. Astrophys. **571**, A16 (2014).
[3] Serguei Chatrchyan *et al.* (CMS Collaboration), Search for dark matter and large extra dimensions in monojet events in pp collisions at $\sqrt{s} = 7$ TeV, J. High Energy Phys. 09 (2012) 094.
[4] Georges Aad *et al.* (ATLAS Collaboration), Search for dark matter candidates and large extra dimensions in events with a jet and missing transverse momentum with the ATLAS detector, J. High Energy Phys. 04 (2013) 075.
[5] R. Agnese *et al.* (SuperCDMS Collaboration), Search for Low-Mass Weakly Interacting Massive Particles with SuperCDMS, Phys. Rev. Lett. **112**, 241302 (2014).
[6] G. Angloher *et al.*, Results from 730 kg days of the CRESST-II dark matter search, Eur. Phys. J. C **72**, 1971 (2012).
[7] M. Felizardo *et al.*, Final Analysis and Results of the Phase II SIMPLE Dark Matter Search, Phys. Rev. Lett. **108**, 201302 (2012).
[8] Michael Klasen, Martin Pohl, and Günter Sigl, Indirect and direct search for dark matter, Prog. Part. Nucl. Phys. **85**, 1 (2015).
[9] D. S. Akerib *et al.* (LUX Collaboration), First Results from the LUX Dark Matter Experiment at the Sanford Underground Research Facility, Phys. Rev. Lett. **112**, 091303 (2014).
[10] Z. Ahmed *et al.* (CDMS-II Collaboration), Results from a Low-Energy Analysis of the CDMS II Germanium Data, Phys. Rev. Lett. **106**, 131302 (2011).
[11] R. Bernabei *et al.* (DAMA, LIBRA Collaborations), New results from DAMA/LIBRA, Eur. Phys. J. C **67**, 39 (2010).
[12] C. E. Aalseth *et al.* (CoGeNT Collaboration), Results from a Search for Light-Mass Dark Matter with a P-type Point Contact Germanium Detector, Phys. Rev. Lett. **106**, 131301 (2011).
[13] E. Aprile *et al.* (XENON100 Collaboration), Dark Matter Results from 225 Live Days of XENON100 Data, Phys. Rev. Lett. **109**, 181301 (2012).
[14] Jan Conrad, Indirect detection of WIMP dark matter: A compact review, in *Interplay between Particle and Astroparticle Physics* (2014), arXiv:1411.1925.
[15] Benjamin W. Lee and Steven Weinberg, Cosmological Lower Bound on Heavy Neutrino Masses, Phys. Rev. Lett. **39**, 165 (1977).
[16] M. I. Vysotsky, A. D. Dolgov, and Ya. B. Zeldovich, Cosmological restriction on neutral lepton masses, JETP Lett. **26**, 188 (1977), https://inspirehep.net/literature/125037.
[17] H. Goldberg, Constraint on the Photino Mass from Cosmology, Phys. Rev. Lett. **50**, 1419 (1983); **103**, 099905(E) (2009).

[18] Gary Steigman and Michael S. Turner, Cosmological constraints on the properties of weakly interacting massive particles, Nucl. Phys. **B253**, 375 (1985).
[19] Paolo Gondolo and Graciela Gelmini, Cosmic abundances of stable particles: Improved analysis, Nucl. Phys. **B360**, 145 (1991).
[20] Gary Steigman, Basudeb Dasgupta, and John F. Beacom, Precise relic WIMP abundance and its impact on searches for dark matter annihilation, Phys. Rev. D **86**, 023506 (2012).
[21] M. Ackermann *et al.* (Fermi-LAT Collaboration), Constraints on the galactic halo dark matter from Fermi-LAT diffuse measurements, Astrophys. J. **761**, 91 (2012).
[22] Teresa Marrodán Undagoitia and Ludwig Rauch, Dark matter direct-detection experiments, J. Phys. G **43**, 013001 (2016).
[23] D. S. Akerib *et al.* (LUX Collaboration), Results from a Search for Dark Matter in the Complete LUX Exposure, Phys. Rev. Lett. **118**, 021303 (2017).
[24] A. Albert *et al.*, Results from the search for dark matter in the Milky Way with 9 years of data of the ANTARES neutrino telescope, Phys. Lett. B **769**, 249 (2017); **796**, 253(E) (2019).
[25] M. L. Ahnen *et al.* (MAGIC, Fermi-LAT Collaborations), Limits to dark matter annihilation cross-section from a combined analysis of MAGIC and Fermi-LAT observations of dwarf satellite galaxies, J. Cosmol. Astropart. Phys. 02 (2016) 039.
[26] E. Aprile *et al.* (XENON Collaboration), First Dark Matter Search Results from the XENON1T Experiment, Phys. Rev. Lett. **119**, 181301 (2017).
[27] C. Amole *et al.* (PICO Collaboration), Dark Matter Search Results from the PICO-60 C_3F_8 Bubble Chamber, Phys. Rev. Lett. **118**, 251301 (2017).
[28] M. G. Aartsen *et al.* (IceCube Collaboration), Search for neutrinos from dark matter self-annihilations in the center of the Milky Way with 3 years of IceCube/DeepCore, Eur. Phys. J. C **77**, 627 (2017).
[29] Xiangyi Cui *et al.* (PandaX-II Collaboration), Dark Matter Results From 54-Ton-Day Exposure of PandaX-II Experiment, Phys. Rev. Lett. **119**, 181302 (2017).
[30] A. Albert *et al.* (HAWC Collaboration), Dark matter limits from dwarf spheroidal galaxies with the HAWC gamma-ray observatory, Astrophys. J. **853**, 154 (2018).
[31] A. U. Abeysekara *et al.* (HAWC Collaboration), A search for dark matter in the galactic halo with HAWC, J. Cosmol. Astropart. Phys. 02 (2018) 049.
[32] H. Abdallah *et al.* (HESS Collaboration), Search for γ-Ray Line Signals from Dark Matter Annihilations in the Inner Galactic Halo from 10 Years of Observations with H.E.S.S., Phys. Rev. Lett. **120**, 201101 (2018).
[33] Fernando Monteiro, Gadi Afek, Daniel Carney, Gordan Krnjaic, Jiaxiang Wang, and David C. Moore, Search for Composite Dark Matter with Optically Levitated Sensors, Phys. Rev. Lett. **125**, 181102 (2020).
[34] Oliver Buchmueller, Caterina Doglioni, and Lian Tao Wang, Search for dark matter at colliders, Nat. Phys. **13**, 217 (2017).
[35] Björn Penning, The pursuit of dark matter at colliders—an overview, J. Phys. G **45**, 063001 (2018).
[36] Salvatore Rappoccio, The experimental status of direct searches for exotic physics beyond the standard model at the Large Hadron Collider, Rev. Phys. **4**, 100027 (2019).
[37] D. Comelli, M. Pietroni, and A. Riotto, Dark energy and dark matter, Phys. Lett. B **571**, 115 (2003).
[38] Orfeu Bertolami, F. Gil Pedro, and M. Le Delliou, Dark energy-dark matter interaction and the violation of the equivalence principle from the Abell Cluster A586, Phys. Lett. B **654**, 165 (2007).
[39] O. Bertolami, F. Gil Pedro, and M. Le Delliou, The Abell Cluster A586 and the equivalence principle, Gen. Relativ. Gravit. **41**, 2839 (2009).
[40] Morgan Le Delliou, Orfeu Bertolami, and Francisco Gil Pedro, Dark energy-dark matter interaction from the Abell Cluster A586 and violation of the equivalence principle, AIP Conf. Proc. **957**, 421 (2007).
[41] E. Abdalla, L. Raul W. Abramo, L. Sodre, Jr., and B. Wang, Signature of the interaction between dark energy and dark matter in galaxy clusters, Phys. Lett. B **673**, 107 (2009).
[42] Orfeu Bertolami, Francisco Gil Pedro, and Morgan Le Delliou, Dark energy-dark matter interaction from the Abell Cluster A586, EAS Publ. Ser. **30**, 161 (2008).
[43] Elcio Abdalla, L. Raul Abramo, and Jose C. C. de Souza, Signature of the interaction between dark energy and dark matter in observations, Phys. Rev. D **82**, 023508 (2010).
[44] Orfeu Bertolami, Francisco Gil Pedro, and Morgan Le Delliou, Testing the interaction of dark energy to dark matter through the analysis of virial relaxation of clusters Abell Clusters A586 and A1689 using realistic density profiles, Gen. Relativ. Gravit. **44**, 1073 (2012).
[45] Morgan Le Delliou, Rafael J. F. Marcondes, Gastao B. Lima Neto, and Elcio Abdalla, Non-virialized clusters for detection of dark energy–dark matter interaction, Mon. Not. R. Astron. Soc. **453**, 2 (2015).
[46] Morgan Le Delliou, Rafael J. F. Marcondes, and Gastão B. Lima Neto, New observational constraints on interacting dark energy using galaxy clusters virial equilibrium states, Mon. Not. R. Astron. Soc. **490**, 1944 (2019).
[47] G. Bertone, D. Hooper, and J. Silk, Particle dark matter: Evidence, candidates and constraints, Phys. Rep. **405**, 279 (2005).
[48] Jonathan L. Feng, Dark matter candidates from particle physics and methods of detection, Annu. Rev. Astron. Astrophys. **48**, 495 (2010).
[49] Eugeny Babichev, Luca Marzola, Martti Raidal, Angnis Schmidt-May, Federico Urban, Hardi Veermäe, and Mikael von Strauss, Bigravitational origin of dark matter, Phys. Rev. D **94**, 084055 (2016).
[50] Katsuki Aoki and Shinji Mukohyama, Massive gravitons as dark matter and gravitational waves, Phys. Rev. D **94**, 024001 (2016).
[51] S. F. Hassan and Rachel A. Rosen, Bimetric gravity from ghost-free massive gravity, J. High Energy Phys. 02 (2012) 126.
[52] Daniel J. H. Chung, Edward W. Kolb, and Antonio Riotto, Superheavy dark matter, Phys. Rev. D **59**, 023501 (1998).
[53] Vadim Kuzmin and Igor Tkachev, Ultrahigh-energy cosmic rays, superheavy long living particles, and matter creation after inflation, JETP Lett. **68**, 271 (1998).

[54] Vadim Kuzmin and Igor Tkachev, Matter creation via vacuum fluctuations in the early Universe and observed ultrahigh-energy cosmic ray events, Phys. Rev. D **59**, 123006 (1999).
[55] Edward W. Kolb, Daniel J. H. Chung, and Antonio Riotto, WIMPzillas!, AIP Conf. Proc. **484**, 91 (1999).
[56] Daniel J. H. Chung, Edward W. Kolb, Antonio Riotto, and Igor I. Tkachev, Probing Planckian physics: Resonant production of particles during inflation and features in the primordial power spectrum, Phys. Rev. D **62**, 043508 (2000).
[57] Vadim A. Kuzmin and Igor I. Tkachev, Ultrahigh-energy cosmic rays and inflation relics, Phys. Rep. **320**, 199 (1999).
[58] Daniel J. H. Chung, Patrick Crotty, Edward W. Kolb, and Antonio Riotto, On the gravitational production of superheavy dark matter, Phys. Rev. D **64**, 043503 (2001).
[59] V. A. Kuzmin and V. A. Rubakov, Ultrahigh-energy cosmic rays: A Window to postinflationary reheating epoch of the Universe?, Phys. At. Nucl. **61**, 1028 (1998).
[60] V. Berezinsky, M. Kachelriess, and A. Vilenkin, Ultrahigh-Energy Cosmic Rays without GZK Cutoff, Phys. Rev. Lett. **79**, 4302 (1997).
[61] Edward W. Kolb, A. A. Starobinsky, and I. I. Tkachev, Trans-Planckian wimpzillas, J. Cosmol. Astropart. Phys. 07 (2007) 005.
[62] Kristjan Kannike, Antonio Racioppi, and Martti Raidal, Super-heavy dark matter—Towards predictive scenarios from inflation, Nucl. Phys. **B918**, 162 (2017).
[63] Brian R. Greene, Tomislav Prokopec, and Thomas G. Roos, Inflaton decay and heavy particle production with negative coupling, Phys. Rev. D **56**, 6484 (1997).
[64] Daniel J. H. Chung, Edward W. Kolb, and Antonio Riotto, Nonthermal Supermassive Dark Matter, Phys. Rev. Lett. **81**, 4048 (1998).
[65] Daniel J. H. Chung, Edward W. Kolb, and Antonio Riotto, Production of massive particles during reheating, Phys. Rev. D **60**, 063504 (1999).
[66] D. S. Gorbunov and A. G. Panin, Scalaron the mighty: Producing dark matter and baryon asymmetry at reheating, Phys. Lett. B **700**, 157 (2011).
[67] Rome Samanta and Federico R. Urban, Testing super heavy dark matter from primordial black holes with gravitational waves, J. Cosmol. Astropart. Phys. 06 (2022) 017.
[68] A. De Rujula, S. L. Glashow, and U. Sarid, Charged dark matter, Nucl. Phys. **B333**, 173 (1990).
[69] John R. Ellis, G. B. Gelmini, Jorge L. Lopez, Dimitri V. Nanopoulos, and Subir Sarkar, Astrophysical constraints on massive unstable neutral relic particles, Nucl. Phys. **B373**, 399 (1992).
[70] Subir Sarkar, Big Bang nucleosynthesis and physics beyond the Standard Model, Rep. Prog. Phys. **59**, 1493 (1996).
[71] Marco Chianese, Damiano F. G. Fiorillo, Rasmi Hajjar, Gennaro Miele, and Ninetta Saviano, Constraints on heavy decaying dark matter with current gamma-ray measurements, J. Cosmol. Astropart. Phys. 11 (2021) 035.
[72] M. Takeda *et al.*, Energy determination in the Akeno Giant Air Shower Array experiment, Astropart. Phys. **19**, 447 (2003).
[73] T. Abu-Zayyad, R. Aida, M. Allen, R. Anderson, R. Azuma, E. Barcikowski, J. W. Belz, D. R. Bergman, S. A. Blake, R. Cady *et al.*, The cosmic-ray energy spectrym observed with the surface detector of the Telescope Array experiment, Astrophys. J. **768**, L1 (2013).
[74] J. Abraham *et al.* (Pierre Auger Collaboration), Observation of the Suppression of the Flux of Cosmic Rays Above 4×10^{19} eV, Phys. Rev. Lett. **101**, 061101 (2008).
[75] M. G. Aartsen *et al.* (IceCube Collaboration), Evidence for high-energy extraterrestrial neutrinos at the IceCube detector, Science **342**, 1242856 (2013).
[76] M. G. Aartsen *et al.* (IceCube Collaboration), Observation of High-Energy Astrophysical Neutrinos in Three Years of IceCube Data, Phys. Rev. Lett. **113**, 101101 (2014).
[77] Kohta Murase, Ranjan Laha, Shin'ichiro Ando, and Markus Ahlers, Testing the Dark Matter Scenario for PeV Neutrinos Observed in IceCube, Phys. Rev. Lett. **115**, 071301 (2015).
[78] Atri Bhattacharya, Mary Hall Reno, and Ina Sarcevic, Reconciling neutrino flux from heavy dark matter decay and recent events at IceCube, J. High Energy Phys. 06 (2014) 110.
[79] Arman Esmaili and Pasquale Dario Serpico, Are IceCube neutrinos unveiling PeV-scale decaying dark matter?, J. Cosmol. Astropart. Phys. 11 (2013) 054.
[80] P. S. Bhupal Dev, D. Kazanas, R. N. Mohapatra, V. L. Teplitz, and Yongchao Zhang, Heavy right-handed neutrino dark matter and PeV neutrinos at IceCube, J. Cosmol. Astropart. Phys. 08 (2016) 034.
[81] Arman Esmaili, Sin Kyu Kang, and Pasquale Dario Serpico, IceCube events and decaying dark matter: Hints and constraints, J. Cosmol. Astropart. Phys. 12 (2014) 054.
[82] Carsten Rott, Kazunori Kohri, and Seong Chan Park, Superheavy dark matter and IceCube neutrino signals: Bounds on decaying dark matter, Phys. Rev. D **92**, 023529 (2015).
[83] M. Yu. Kuznetsov, Hadronically decaying heavy dark matter and high-energy neutrino limits, JETP Lett. **105**, 561 (2017).
[84] Timothy Cohen, Kohta Murase, Nicholas L. Rodd, Benjamin R. Safdi, and Yotam Soreq, γ -ray Constraints on Decaying Dark Matter and Implications for IceCube, Phys. Rev. Lett. **119**, 021102 (2017).
[85] Brian Feldstein, Alexander Kusenko, Shigeki Matsumoto, and Tsutomu T. Yanagida, Neutrinos at IceCube from heavy decaying dark matter, Phys. Rev. D **88**, 015004 (2013).
[86] Nagisa Hiroshima, Ryuichiro Kitano, Kazunori Kohri, and Kohta Murase, High-energy neutrinos from multibody decaying dark matter, Phys. Rev. D **97**, 023006 (2018).
[87] Alexander Aab *et al.* (Pierre Auger Collaboration), Observation of a large-scale anisotropy in the arrival directions of cosmic rays above 8×10^{18} eV, Science **357**, 1266 (2017).
[88] Alexander Aab *et al.* (Pierre Auger Collaboration), An indication of anisotropy in arrival directions of ultra-high-energy cosmic rays through comparison to the flux pattern of extragalactic gamma-ray sources, Astrophys. J. Lett. **853**, L29 (2018).

[89] Esteban Alcantara, Luis A. Anchordoqui, and Jorge F. Soriano, Hunting for superheavy dark matter with the highest-energy cosmic rays, Phys. Rev. D **99**, 103016 (2019).
[90] Gustavo A. Medina-Tanco and A. A. Watson, Dark matter halos and the anisotropy of ultrahigh-energy cosmic rays, Astropart. Phys. **12**, 25 (1999).
[91] R. Aloisio and F. Tortorici, Super heavy dark matter and UHECR anisotropy at low energy, Astropart. Phys. **29**, 307 (2008).
[92] Oleg E. Kalashev, B. A. Khrenov, P. Klimov, S. Sharakin, and Sergey V. Troitsky, Global anisotropy of arrival directions of ultrahigh-energy cosmic rays: Capabilities of space-based detectors, J. Cosmol. Astropart. Phys. 03 (2008) 003.
[93] R. Aloisio, S. Matarrese, and A. V. Olinto, Super heavy dark matter in light of BICEP2, Planck and ultra high energy cosmic rays observations, J. Cosmol. Astropart. Phys. 08 (2015) 024.
[94] O. E. Kalashev and M. Yu Kuznetsov, Heavy decaying dark matter and large-scale anisotropy of high-energy cosmic rays, JETP Lett. **106**, 73 (2017).
[95] Luca Marzola and Federico R. Urban, Ultra high energy cosmic rays & super-heavy dark matter, Astropart. Phys. **93**, 56 (2017).
[96] B. P. Abbott *et al.* (LIGO Scientific, Virgo Collaborations), Observation of Gravitational Waves from a Binary Black Hole Merger, Phys. Rev. Lett. **116**, 061102 (2016).
[97] B. P. Abbott *et al.* (LIGO Scientific, Virgo Collaborations), GW151226: Observation of Gravitational Waves from a 22-Solar-Mass Binary Black Hole Coalescence, Phys. Rev. Lett. **116**, 241103 (2016).
[98] Benjamin P. Abbott *et al.* (LIGO Scientific, VIRGO Collaborations), GW170104: Observation of a 50-Solar-Mass Binary Black Hole Coalescence at Redshift 0.2, Phys. Rev. Lett. **118**, 221101 (2017); **121**, 129901(E) (2018).
[99] B. P. Abbott *et al.* (LIGO Scientific, Virgo Collaborations), GW170608: Observation of a 19-solar-mass binary black hole coalescence, Astrophys. J. Lett. **851**, L35 (2017).
[100] B. P. Abbott *et al.* (LIGO Scientific, Virgo Collaborations), GW170814: A Three-Detector Observation of Gravitational Waves from a Binary Black Hole Coalescence, Phys. Rev. Lett. **119**, 141101 (2017).
[101] B. P. Abbott *et al.* (LIGO Scientific, Virgo Collaborations), GW170817: Observation of Gravitational Waves from a Binary Neutron Star Inspiral, Phys. Rev. Lett. **119**, 161101 (2017).
[102] R. Abbott *et al.* (LIGO Scientific, Virgo Collaborations), GW190814: Gravitational waves from the coalescence of a 23 solar mass black hole with a 2.6 solar mass compact object, Astrophys. J. Lett. **896**, L44 (2020).
[103] Michele Maggiore, Gravitational wave experiments and early universe cosmology, Phys. Rep. **331**, 283 (2000).
[104] Joseph D. Romano and Neil J. Cornish, Detection methods for stochastic gravitational-wave backgrounds: A unified treatment, Living Rev. Relativity **20**, 2 (2017).
[105] Chiara Caprini and Daniel G. Figueroa, Cosmological backgrounds of gravitational waves, Classical Quantum Gravity **35**, 163001 (2018).
[106] Nelson Christensen, Stochastic gravitational wave backgrounds, Rep. Prog. Phys. **82**, 016903 (2019).
[107] John R. Ellis, Jorge L. Lopez, and Dimitri V. Nanopoulos, Confinement of fractional charges yields integer charged relics in string models, Phys. Lett. B **247**, 257 (1990).
[108] E. V. Arbuzova, Superheavy dark matter in R^2-cosmology, Int. J. Mod. Phys. D **30**, 2140002 (2021).
[109] Dmitry S. Gorbunov and Valery A. Rubakov, *Introduction to the Theory of the Early Universe: Cosmological Perturbations and Inflationary Theory* (World Scientific Publishing Company, 2011), 10.1142/7873.
[110] O. K. Kalashev and M. Yu. Kuznetsov, Constraining heavy decaying dark matter with the high energy gamma-ray limits, Phys. Rev. D **94**, 063535 (2016).
[111] Kohta Murase and John F. Beacom, Constraining very heavy dark matter using diffuse backgrounds of neutrinos and cascaded gamma rays, J. Cosmol. Astropart. Phys. 10 (2012) 043.
[112] Arman Esmaili and Pasquale Dario Serpico, Gamma-ray bounds from EAS detectors and heavy decaying dark matter constraints, J. Cosmol. Astropart. Phys. 10 (2015) 014.
[113] M. Kachelriess, O. E. Kalashev, and M. Yu. Kuznetsov, Heavy decaying dark matter and IceCube high energy neutrinos, Phys. Rev. D **98**, 083016 (2018).
[114] *The Pierre Auger Observatory: Contributions to the 35th International Cosmic Ray Conference (ICRC 2017)*, edited by Darko Veberic (2017), arXiv:1708.06592.
[115] Andres Romero-Wolf (ZAP Collaboration), The Zettavolt Askaryan Polarimeter (ZAP) mission concept: radio detection of ultra-high energy cosmic rays in low lunar orbit, Proc. Sci., ICRC2021 (2021) 403.
[116] Roberto Aloisio, V. Berezinsky, and M. Kachelriess, On the status of superheavy dark matter, Phys. Rev. D **74**, 023516 (2006).
[117] P. Sommers, Cosmic ray anisotropy analysis with a full-sky observatory, Astropart. Phys. **14**, 271 (2001).
[118] Alexander Aab *et al.* (Telescope Array, Pierre Auger Collaborations), Searches for large-scale anisotropy in the arrival directions of cosmic rays detected above energy of 10^{19} eV at the pierre auger observatory and the telescope array, Astrophys. J. **794**, 172 (2014).
[119] J. Abraham *et al.*, Properties and performance of the prototype instrument for the pierre auger observatory, Nucl. Instrum. Methods Phys. Res., Sect. A **523**, 50 (2004).
[120] Lino Miramonti, Latest results and future prospects of the pierre auger observatory, J. Phys. **1766**, 012002 (2021).
[121] Julio F. Navarro, Carlos S. Frenk, and Simon D. M. White, The structure of cold dark matter halos, Astrophys. J. **462**, 563 (1996).
[122] J. Einasto, On the construction of a composite model for the galaxy and on the determination of the system of galactic parameters, Tr. Astrofiz. Inst. Alma-Ata **5**, 87 (1965), https://ui.adsabs.harvard.edu/abs/1965TrAlm...5...87E/abstract.
[123] Alister W. Graham, David Merritt, Ben Moore, Juerg Diemand, and Balsa Terzic, Empirical models for dark matter halos. I. Nonparametric construction of density

profiles and comparison with parametric models, Astron. J. **132**, 2685 (2006).
[124] Julio F. Navarro, Aaron Ludlow, Volker Springel, Jie Wang, Mark Vogelsberger, Simon D. M. White, Adrian Jenkins, Carlos S. Frenk, and Amina Helmi, The diversity and similarity of cold dark matter halos, Mon. Not. R. Astron. Soc. **402**, 21 (2010).
[125] Pablo F. de Salas and Axel Widmark, Dark matter local density determination: Recent observations and future prospects, Rep. Prog. Phys. **84**, 104901 (2021).
[126] A. D. Supanitsky and G. Medina-Tanco, Ultra high energy cosmic rays from super-heavy dark matter in the context of large exposure observatories, J. Cosmol. Astropart. Phys. 11 (2019) 036.
[127] S. L. Dubovsky and P. G. Tinyakov, Galactic anisotropy as signature of CDM related ultrahigh-energy cosmic rays, JETP Lett. **68**, 107 (1998).
[128] N. Wyn Evans, Francesc Ferrer, and Subir Sarkar, The anisotropy of the ultrahigh-energy cosmic rays, Astropart. Phys. **17**, 319 (2002).
[129] Lars Bergstrom, Piero Ullio, and James H. Buckley, Observability of gamma-rays from dark matter neutralino annihilations in the Milky Way halo, Astropart. Phys. **9**, 137 (1998).
[130] Argyro Tasitsiomi and A. V. Olinto, Detectability of neutralino clumps via atmospheric Cherenkov telescopes, Phys. Rev. D **66**, 083006 (2002).
[131] Torsten Bringmann, Lars Bergstrom, and Joakim Edsjo, New gamma-ray contributions to supersymmetric dark matter annihilation, J. High Energy Phys. 01 (2008) 049.
[132] Francesca Calore, Valentina De Romeri, Mattia Di Mauro, Fiorenza Donato, and Federico Marinacci, Realistic estimation for the detectability of dark matter subhalos with Fermi-LAT, Phys. Rev. D **96**, 063009 (2017).
[133] Francisco Pedreira (Pierre Auger Collaboration), Bounds on diffuse and point source fluxes of ultra-high energy neutrinos with the Pierre Auger Observatory, Proc. Sci., ICRC2019 (2021) 979.
[134] Anupam Mazumdar and Graham White, Review of cosmic phase transitions: their significance and experimental signatures, Rep. Prog. Phys. **82**, 076901 (2019).
[135] T. W. B. Kibble, Topology of cosmic domains and strings, J. Phys. A **9**, 1387 (1976).
[136] Rachel Jeannerot, Jonathan Rocher, and Mairi Sakellariadou, How generic is cosmic string formation in SUSY GUTs, Phys. Rev. D **68**, 103514 (2003).
[137] H. B. Nielsen and P. Olesen, Vortex-line models for dual strings, Nucl. Phys. **B61**, 45 (1973).
[138] Tanmay Vachaspati and Alexander Vilenkin, Gravitational radiation from cosmic strings, Phys. Rev. D **31**, 3052 (1985).
[139] Pierre Auclair, Jose J. Blanco-Pillado, Daniel G. Figueroa, Alexander C. Jenkins, Marek Lewicki, Mairi Sakellariadou, Sotiris Sanidas, Lara Sousa, Danièle A. Steer, Jeremy M. Wachter, and Sachiko Kuroyanagi, Probing the gravitational wave background from cosmic strings with LISA, J. Cosmol. Astropart. Phys. 04 (2020) 034.
[140] Zaven Arzoumanian *et al.* (NANOGrav Collaboration), The NANOGrav 12.5 yr data set: Search for an isotropic stochastic gravitational-wave background, Astrophys. J. Lett. **905**, L34 (2020).
[141] L. Lentati *et al.*, European pulsar timing array limits on an isotropic stochastic gravitational-wave background, Mon. Not. R. Astron. Soc. **453**, 2576 (2015).
[142] Z. Arzoumanian *et al.* (NANOGRAV Collaboration), The NANOGrav 11-year data set: Pulsar-timing constraints on the stochastic gravitational-wave background, Astrophys. J. **859**, 47 (2018).
[143] Ligong Bian, Xuewen Liu, and Ke-Pan Xie, Probing superheavy dark matter with gravitational waves, J. High Energy Phys. 11 (2021) 175.
[144] Simone Blasi, Vedran Brdar, and Kai Schmitz, Has NANOGrav Found First Evidence for Cosmic Strings?, Phys. Rev. Lett. **126**, 041305 (2021).
[145] M. Torki, H. Hajizadeh, M. Farhang, A. Vafaei Sadr, and S. M. S. Movahed, Planck limits on cosmic string tension using machine learning, Mon. Not. R. Astron. Soc. **509**, 2169 (2021).
[146] Pau Amaro-Seoane *et al.* (LISA Collaboration), Laser interferometer space antenna, arXiv:1702.00786.
[147] Vincent Corbin and Neil J. Cornish, Detecting the cosmic gravitational wave background with the big bang observer, Classical Quantum Gravity **23**, 2435 (2006).
[148] Teresa Bister, Anisotropies in the arrival directions of ultra-high-energy cosmic rays measured at the pierre auger observatory, Phys. Scr. **96**, 074003 (2021).
[149] Mathias Garny, McCullen Sandora, and Martin S. Sloth, Planckian Interacting Massive Particles as Dark Matter, Phys. Rev. Lett. **116**, 101302 (2016).
[150] Daniel J. H. Chung, Edward W. Kolb, Antonio Riotto, and Leonardo Senatore, Isocurvature constraints on gravitationally produced superheavy dark matter, Phys. Rev. D **72**, 023511 (2005).
[151] P. A. R. Ade *et al.* (Planck Collaboration), Planck 2015 results. XX. Constraints on inflation, Astron. Astrophys. **594**, A20 (2016).
[152] P. A. R. Ade *et al.* (BICEP2, Keck Array Collaborations), Improved Constraints on Cosmology and Foregrounds from BICEP2 and Keck Array Cosmic Microwave Background Data with Inclusion of 95 GHz Band, Phys. Rev. Lett. **116**, 031302 (2016).
[153] D. S. Gorbunov and A. G. Panin, Free scalar dark matter candidates in R^2-inflation: The light, the heavy and the superheavy, Phys. Lett. B **718**, 15 (2012).
[154] Oleg E. Kalashev, G. I. Rubtsov, and Sergey V. Troitsky, Sensitivity of cosmic-ray experiments to ultra-high-energy photons: Reconstruction of the spectrum and limits on the superheavy dark matter, Phys. Rev. D **80**, 103006 (2009).